Time-Dependent Infrared Emission Following Photodissociation of Nitromethane and Chloropicrin

Elisabeth A. Wade,* Kristina E. Reak, and Sissi L. Li

Department of Chemistry & Physics, Mills College, Oakland, California 94613

Samuel M. Clegg,† Peng Zou, and David L. Osborn

Combustion Research Facility, Sandia National Laboratories, Livermore, California 94551

Received: August 10, 2005; In Final Form: January 3, 2006

Nitromethane (CH_3NO_2) and its chlorinated analogue, chloropicrin (CCl_3NO_2), were photolyzed at 193, 248, and 266 nm, and the products were observed by time-dependent Fourier transform infrared emission spectroscopy. At 193 and 248 nm, the primary photodissociation pathway for nitromethane was cleavage of the C−N bond to produce CH_3 + $NO_2(\tilde{A}\ ^2B_2)$. At 266 nm, weak emission was observed following photodissociation of nitromethane, but an infrared spectrum could not be obtained. The photodissociation of chloropicrin at 193 nm produced the analogous product channel CCl_3 + $NO_2(\tilde{A}\ ^2B_2)$ in addition to several other product channels. At 248 and 266 nm, only CCl_3 + $NO_2(\tilde{A}\ ^2B_2)$ was observed. The production of phosgene (CCl_2O) from chloropicrin photodissociation was not observed in this study.

Introduction

The spectroscopy and photochemistry of nitromethane (CH_3NO_2) has been of interest for nearly half a century.[1−6,8−20] Nitromethane's absorption spectrum consists of two broad bands: a weak $\pi^* \leftarrow n$ transition centered at 270 nm[1] and a much stronger $\pi^* \leftarrow \pi$ transition centered at 198 nm,[2] as shown in Figure 1. Either of these transitions can lead to dissociation through several energetically accessible channels, including cleavage of the C−N bond to produce a methyl radical and nitrogen dioxide

$$CH_3NO_2 \rightarrow CH_3 + NO_2 \qquad (1)$$

and molecular elimination to produce formaldehyde and HNO.

$$CH_3NO_2 \rightarrow CH_2O + HNO \qquad (2)$$

These channels are shown schematically in Figure 2.

Several groups have studied the photodissociation of nitromethane following 193 nm irradiation of the strong $\pi^* \leftarrow \pi$ transition. Blais[3] measured the dissociation cross-section of channel 1 (C−N bond fission) as 1.7×10^{-17} cm^2 and determined a quantum yield near unity. Butler et al.[4] used fluorescence emission spectroscopy and photofragment translational spectroscopy to follow the reaction products when nitromethane was photodissociated in a molecular beam. They showed that the primary process was cleavage of the C−N bond and further suggested that there were two competing channels. The major channel produced NO_2 in the first electronically excited state ($\tilde{A}\ ^2B_2$), with some (>10%) of this NO_2 containing sufficient internal energy for unimolecular dissociation to NO + O. A second, minor channel produced NO_2 ($\tilde{X}\ ^2A_1$) with little translational energy and a strong propensity for absorbing a second 193 nm photon, leading to photodissociation of NO_2 to NO + O.[4] Lao et al.[5] observed resolved emission spectra following excitation at 200 and 218 nm and used the distribution of the emission intensity to characterize the dissociation dynamics. They also reinterpreted the minor channel observed by Butler et al.,[4] suggesting that it occurred via near-threshold dissociation of nitromethane to produce NO_2 ($2\ ^2B_2$) with less than 2 kcal/mol of excess energy. Moss et al.[6] used REMPI and time-of-flight mass spectroscopy to determine nascent photofragment energy distributions for the photoproducts of 193 nm nitromethane photodissociation. The results of Lao et al.[5] and Moss et al.[6] are consistent with the dissociation mechanism proposed by Butler et al.[4] Note that there are multiple notations used for the electronically excited states of NO_2; the first excited state is identified as $\tilde{A}\ ^2B_2$ by Butler et al.[4] and as $1\ ^2B_2$ by Moss et al.[6] In this work, we will use the same notation as Butler et al.[4] and Delon and Jost.[7]

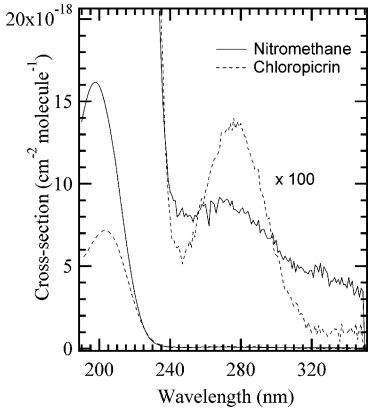

Figure 1. Ultraviolet absorption spectra of nitromethane (solid line) and chloropicrin (dotted line) with cross-sections in base *e*. The weak $\pi^* \leftarrow n$ transition at ∼270 nm is magnified by a factor of 100.

Studies of the photodissociation of nitromethane following excitation of the weak $\pi^* \leftarrow n$ transition have produced less

* To whom correspondence should be addressed. E-mail: ewade@mills.edu.

† Permanent address: Los Alamos National Laboratory, Los Alamos, NM 87545.

10.1021/jp054480y CCC: $33.50
Published on Web 03/09/2006

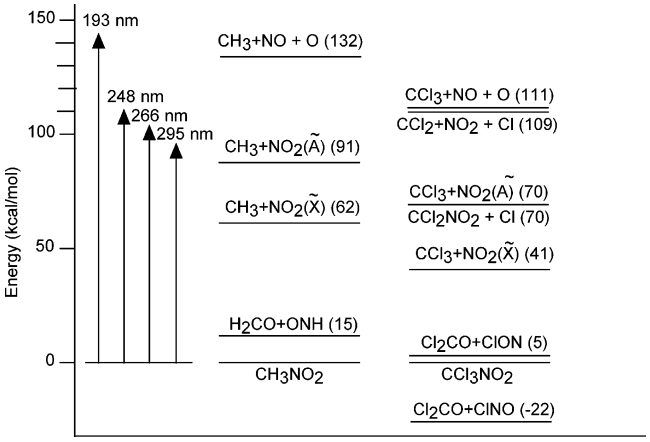

Figure 2. Schematic representation of some energetically allowed dissociation channels for nitromethane and chloropicrin. The nitromethane channel energies are calculated using heats of formation taken from webbook.nist.gov.[35] The chloropicrin channel energies are calculated using Gaussian 98[31] at the CBS-Q level of theory, including zero-point energy.[36]

consistent results. Spears and Brugge[8] dissociated nitromethane at 252.6 nm and observed vibrationally excited NO_2. Kwok et al.[9] observed no photodissociation when nitromethane was excited at 266 nm under collision-free conditions. Schoen et al.[10] observed the formation of ground state NO_2 when photodissociating nitromethane with a picosecond laser at 264 nm. Zabarnick et al.[11] observed a small yield of OH radicals when nitromethane was photodissociated at 266 nm. Greenblatt et al.[12] observed no OH production at 282 nm. Park et al.[13] studied the dynamics of oxygen atom formation following 248 and 266 nm photodissociation of nitromethane and determined that the oxygen atoms were formed by an indirect mechanism at both 248 and 266 nm but that there was an additional direct predissociation mechanism at 248 nm. In the Discussion, we discuss our results in the context of these varied observations.

Considering the number of experimental studies of nitromethane, there has been relatively little theoretical work on this system. Several groups have performed calculations on the ground state potential energy surface (PES) and the thermal decomposition of nitromethane,[14−17] but to our knowledge, there are only four studies dealing with the electronically excited states important in photodissociation. Mijoule et al.[18] studied the first excited singlet states at the SCF + CI level of theory and found that all of the excited states studied were strongly predissociative. Roszak and Kaufman[19] studied the low-lying excited singlet and triplet PESs for the decomposition of nitromethane at the multireference double-excitation configuration-interaction level. They found that only the first A″ singlet state is predissociative, whereas two A′ singlet states are stable and a second A″ singlet state is repulsive. Most recently, Arenas et al.[20,21] have specifically studied the ground and excited state PESs of nitromethane as they relate to photodissociation at 193 nm. Their original calculations in 2003[20] predicted that nitromethane dissociates following two channels: a major channel consisting of excitation to the 2A″ state, internal conversion to the 2A′ state, and dissociation to produce $CH_3 + NO_2$ ($\tilde{B}\ ^2B_1$), and a minor channel where the initially excited 2A″ state directly dissociates to produce $CH_3 + NO_2$ ($\tilde{C}\ ^2A_2$). However, their more recent work in 2005[21] proposes a radiationless decay through a conical intersection, which deactivates the electronically excited nitromethane and causes it to dissociate and form $CH_3 + NO_2$ ($\tilde{A}\ ^2B_2$), as is consistent with the assignments of Butler et al.[4]

Chloropicrin (CCl_3NO_2, trichloronitromethane) is the chlorinated analogue of nitromethane. Its spectrum is very similar to that of nitromethane, as shown in Figure 1. The band at 200 nm is weaker than that of nitromethane, while the weak band at 280 nm is stronger. Chloropicrin is an agricultural pesticide that can escape into the atmosphere after application,[22] and its primary environmental removal pathway is photolysis.[23] Because of the similarity of its ultraviolet spectrum to that of nitromethane,[24] it might be reasonable to predict that chloropicrin's photolysis mechanism would be comparable to that of nitromethane. However, the earliest study of the environmental removal of chloropicrin, by Moilanen et al.,[25] suggested that chloropicrin did not photolyze in the absence of oxygen. In contrast, more recent studies have shown that chloropicrin does photolyze independently. Carter et al.[26] measured the quantum yield for production of Cl atoms and NO_x from chloropicrin at ppb concentrations in air from 270 to 390 nm. For photolysis with simulated sunlight at 1 atm total pressure, they found the photodecomposition quantum yield to be 0.87 ± 0.26. These measurements were performed at long times, after ∼6 h of irradiation, so that secondary chemistry was significant. They also performed kinetic modeling studies of the reactions of chloropicrin with various organic pollutants, and these models suggested that the primary dissociation mechanism was cleavage of the C−N bond.[26] Wade et al.[27] studied the photolysis of chloropicrin in cryogenic matrices, monitoring the reaction via infrared absorption spectroscopy, and found that the final photolysis products were phosgene (Cl_2CO) and nitrosyl chloride (ClNO). The kinetic data also suggested that at least some, and perhaps all, of the phosgene and nitrosyl chloride were secondary photoproducts, which may also support cleavage of the C−N bond as the primary dissociation step. However, in that experiment, the likely primary photoproducts, NO_2 and CCl_3, could not be observed directly as their infrared bands overlapped with strong infrared bands in chloropicrin.[27]

In this experiment, we use time-resolved Fourier transform infrared (FTIR) spectroscopy to observe the infrared emission following photodissociation of nitromethane and chloropicrin at 193, 248, and 266 nm. By observing emission rather than absorption, we minimize interference between product and parent infrared bands.

Experimental Section

The experimental system used here has been described elsewhere.[28] Molecular emission from a room temperature flow cell containing multipass collection optics was modulated by a time-resolved Fourier transform spectrometer, operating in step-scan mode. Calibrated mass flow controllers delivered nitromethane or chloropicrin seeded in helium buffer gas to the flow cell, for a total flow rate of ∼100 standard cm^3/min (sccm). Helium was bubbled through neat chloropicrin or nitromethane, which was held in an ice bath to keep the vapor pressure constant (6.0 Torr for chloropicrin; 9.3 Torr for nitromethane). The total pressure in the bubbler was 400−700 Torr, so the gas flowing into the cell was typically 1−2% nitromethane or chloropicrin. A 100−200 sccm flow of helium purged the photolysis laser windows. The total pressure in the cell was typically 350−400 mTorr. An unfocused ArF laser was used as the 193 nm photodissociation source (30 Hz; 20 mJ cm^{-2} $pulse^{-1}$), an unfocused KrF laser was used as the 248 nm photodissociation source (30 Hz; 55 mJ cm^{-2} $pulse^{-1}$), and the unfocused fourth harmonic of a Nd:YAG laser was used as the 266 nm photodissociation source (10 Hz; 150 mJ cm^{-2} $pulse^{-1}$). In some experiments, the Nd:YAG laser was expanded using a telescope to double the beam diameter, reducing the fluence to 38 mJ cm^{-2} $pulse^{-1}$.

Following the photodissociation pulse, infrared emission was collected perpendicular to the photodissociation laser pulse by a pair of 10 cm diameter silver-coated f/1 spherical mirrors, separated by 20 cm.[28] These multipass collection optics focused the emission to the small area required for fast infrared detectors. The emission passed through a Bruker IFS 66v/S Step-Scan Fourier transform spectrometer, operating in step-scan mode. The modulated emission was then detected using one of three detectors: a HgCdTe photovoltaic detector, sensitive above 800 cm^{-1}; a higher sensitivity InSb detector, sensitive above 1850 cm^{-1}; or a Si photodiode, sensitive above 9000 cm^{-1}. Unless otherwise noted, all spectra shown and discussed below were collected with the HgCdTe detector. In some spectra, filters were used to limit the detected infrared emission to particular regions of the spectra. We use two transient digitizers: a 12-bit, 40 MS/s digitizer configured to collect one interferogram every 250 ns and a 16-bit, 200 kS/s digitizer that collected one interferogram every 5 μs, which was used for all of the data presented in the figures. At 5 μs per interferogram, the sampling rate of the lower-noise 16-bit digitizer was not sufficient to smoothly follow the detector rise times. To ensure some sensitivity to processes occurring on time scales < 5 μs, we adjusted the photodissociation laser delay with respect to digitization (Δt) such that the $\Delta t = 0$ interferogram was collected on the rising edge of the total emission signal, leading to a temporal instrument response function of $\sim$5 μs when the 16-bit digitizer was used. Therefore, molecular emission from photodissociation that occurred on a time scale $\ll 5$ μs appeared to increase during the first 5 μs. We could confirm prompt production of photofragments, albeit with decreased signal-to-noise, using the faster 12-bit digitizer.

Ultraviolet absorbance spectra of nitromethane and chloropicrin, shown in Figure 1, were measured in a 10.2 cm cell using a Hach UV−vis spectrophotometer. Absorption cross-sections of CH_3NO_2 and CCl_3NO_2 are reported in base *e*.

Results

193 nm Photodissociation. Time-resolved spectra of photofragments in a collisional environment provide important clues to the origin of each fragment. In particular, we wish to separate nascent photofragments, which reflect the photodissociation mechanism, from those excited by energy transfer processes or chemical reactions. In the limit that photodissociation is much faster than our detector's rise time, emission from nascent photofragments should rise abruptly and decrease monotonically with time, while emission from molecules excited by other pathways should show a slower increase with time. In addition, to be certain that we were observing products from single photon processes, we performed several power dependence studies of emission following chloropicrin and nitromethane photodissociation. In all cases, the emission showed a first-order dependence on laser power, indicating that the effects observed are not due to multiphoton processes. Note that the photon fluence at 193 nm in this study ($\sim$20 mJ cm^{-2} $pulse^{-1}$) is significantly lower than the $\sim$1 J cm^{-2} $pulse^{-1}$ employed in the studies of Blais[3] and Butler et al.[4]

For both nitromethane and chloropicrin photodissociation at 193 nm, the most intense emission is a broad unstructured band extending from 3500 to 12000 cm^{-1} that appears with a detector-limited rise time and diminishes with a pressure-dependent decay time of $\sim$15 μs under the conditions shown in Figure 3. These survey spectra, taken with the HgCdTe detector, are not corrected for the instrument response function, which causes a decrease in intensity with increasing wavenumber and an artificial dip in intensity near 8200 cm^{-1}. In reality, this band extends from $\sim$3500 to more than 30000 cm^{-1}, as verified in spectra obtained with InSb and Si photodiode detectors combined with CaF_2 and Quartz beam splitters. Emission from this band could also be seen by eye as a pale yellow flash. Its intensity, wavenumber range, and relatively fast quenching (radiative and collisional) are strong evidence that this band arises from an electronic transition. We assign this emission to the $NO_2[(\tilde{A}\ ^2B_2) \rightarrow (\tilde{X}\ ^2A_1)]$ transition,[29] as previously observed by Butler et al.[4] Our observed lifetime for this emission is consistent with $NO_2[(\tilde{A}\ ^2B_2) \rightarrow (\tilde{X}\ ^2A_1)]$, which has a lifetime of 15−200 μs, depending on pressure and excitation conditions.[30]

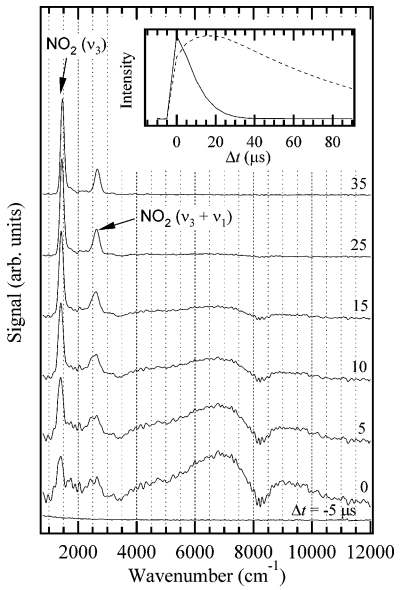

Figure 3. Infrared emission spectra at 64 cm^{-1} resolution following 193 nm photolysis of 6 mTorr nitromethane in He at a total pressure of 391 mTorr, detected with a HgCdTe photodiode. The spectra are not corrected for instrument response. The dip in intensity near 8200 cm^{-1} arises from a node in Ge/KBr beam splitter efficiency. The inset shows temporal profiles of the spectra integrated from 1260 to 1540 cm^{-1} (···) and from 3350 to 12000 cm^{-1} (—).

This emission is less likely to arise from the $(\tilde{B}\ ^2B_1)$ state, as suggested in the 2003 theoretical study by Arenas et al.,[20] because it is experimentally known that the $NO_2[(\tilde{B}\ ^2B_1) \rightarrow (\tilde{X}\ ^2A_1)]$ transition is significantly weaker and should display a structured (0, *n*, 0) progression,[7] which is not observed. Furthermore, Lao et al.[5] observed a structured progression in the NO_2 symmetric stretch, which is unlikely to be due to emission from the $(\tilde{B}\ ^2B_1)$ state.[5] In this work, we shall identify the excited electronic state as $NO_2(\tilde{A}\ ^2B_2)$ but recognize that some NO_2 might be produced in the $(\tilde{B}\ ^2B_1)$ state as well.

Note that the maximum intensity of this electronic transition occurs in our earliest spectrum, and its intensity decreases monotonically with time, suggesting that $NO_2(\tilde{A}\ ^2B_2)$ is a nascent product of photodissociation. For both nitromethane and chloropicrin, the decay of this broad, electronic emission is correlated with the rise of two midinfrared bands at $\sim$1400 and $\sim$2700 cm^{-1}. The inset of Figure 3 demonstrates this correlation, showing the temporal behavior of the $NO_2[(\tilde{A}\ ^2B_2) \rightarrow (\tilde{X}\ ^2A_1)]$ emission as compared to that of the band near 1400 cm^{-1}. In all spectra, the decrease of intensity at long time is due to a combination of emitters leaving the observation zone, loss due to deactivation to a nonemitting state, and loss due to chemical reaction. Accurate assignment of these two mid-IR bands requires better spectral resolution.

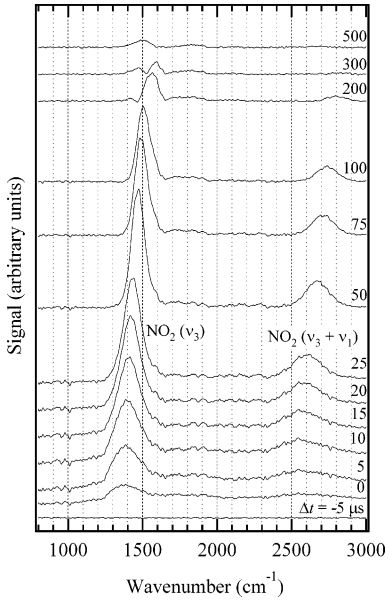

Figure 4. Midinfrared emission spectra at 8 cm^{-1} resolution following 193 nm photolysis of nitromethane, detected with a HgCdTe detector. Pressures are the same as in Figure 3.

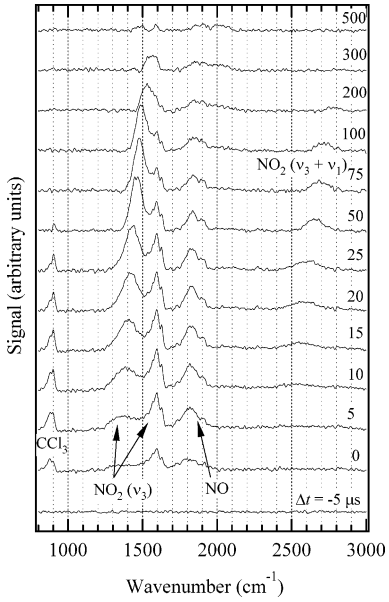

Figure 5. Midinfrared emission spectra at 8 cm^{-1} resolution following 193 nm photolysis of 6 mTorr chloropicrin in He at a total pressure of 474 mTorr, detected with a HgCdTe detector.

Figures 4 and 5 show spectra at 8 cm^{-1} resolution of the mid-infrared emission following 193 nm photodissociation of nitromethane and chloropicrin, respectively. The nitromethane spectra in Figure 4 show the same two mid-IR bands observed at lower resolution in Figure 3. Both bands shift to higher energy with increasing time and are assigned by their asymptotic frequencies to the ν_3 (1618 cm^{-1}) and $\nu_3 + \nu_1$ (2906 cm^{-1}) bands of $NO_2(\tilde{X}^2A_1)$.[7] The observation that these bands at early times are anharmonically red-shifted from their fundamental frequencies is evidence of substantial vibrational excitation in the NO_2 fragment. Vibrational energy transfer due to collisions with the bath gas cools the NO_2, leading to blue-shifting spectra with increasing time. Note that the intensities of both bands in Figure 4 rise with time before decreasing, suggesting that $NO_2(\tilde{X}^2A_1)$ is not a nascent dissociation product for nitromethane. The temporal correlation between the decrease of the electronic emission and the increase of the highly excited

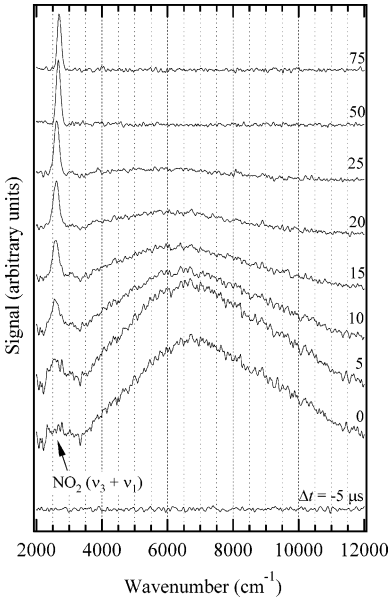

Figure 6. Infrared emission spectra at 32 cm^{-1} resolution following 248 nm photolysis of 7 mTorr chloropicrin in He at a total pressure of 393 mTorr, detected with an InSb detector and a Si/CaF_2 beam splitter.

ν_3 and $\nu_3 + \nu_1$ bands (see Figure 3) is strong evidence that these bands arise from electronic to vibrational quenching of the $NO_2(\tilde{A}\ ^2B_2)$ photofragment. We have not observed emission from the CH_3 cofragment.

The midinfrared emission spectrum for chloropicrin photodissociation in Figure 5 is more complex, showing three additional bands. The ν_3 and $(\nu_3 + \nu_1)$ bands of $NO_2(\tilde{X}^2A_1)$ are still observed near 1400 and 2700 cm^{-1}, with similar temporal profiles as in nitromethane photodissociation. The decay of electronic emission from $NO_2(\tilde{A}\ ^2B_2)$ (not shown) again correlates with the rise of these two bands. In addition, prompt emission at ~900 cm^{-1} in Figure 5 is assigned to the C−Cl stretch of the CCl_3 fragment ($\nu_4 = 898$ cm^{-1}).[32] Together, these observations support a C−N bond cleavage product channel that produces $NO_2(\tilde{A}\ ^2B_2)$, just as in nitromethane.

However, Figure 5 shows an additional band near 1600 cm^{-1} with a detector-limited rise time that can be unambiguously assigned to the ν_3 band of $NO_2(\tilde{X}^2A_1)$. The prompt appearance of this band was confirmed by emission spectra collected with the faster 12-bit digitizer, which collects a spectrum every 250 ns. The minimum in this band, between the P and the R branches of the rotational contour, occurs at 1618 ± 2 cm^{-1}, as expected for the $\nu_3 = 1 \rightarrow 0$ band.[7] This band has a negligible blue shift with time and is eventually subsumed under the more intense, blue-shifting NO_2 ν_3 band that originates near 1400 cm^{-1}. The genesis of these different vibrational distributions is discussed in the Discussion. The final feature observed in Figure 5 is the band that at $\Delta t = 5$ μs lies between 1700 and 1920 cm^{-1}. This band is assigned to NO and shows excitation in the first few vibrational levels. Again, the minimum between the P and the R branches (the Q branch of NO is fairly weak) is observed as expected at 1876 ± 2 cm^{-1}, confirming the assignment to NO.[33] This assignment is further confirmed by spectra taken at 0.1 cm^{-1} resolution, where the rotational structure of NO is clearly resolved. This region of the spectra will be discussed in more detail in the Discussion.

248 nm Photodissociation. Figure 6 shows emission following 248 nm photodissociation of chloropicrin, detected with the InSb photodiode and a Si/CaF_2 beam splitter. This experimental configuration has significantly greater sensitivity than

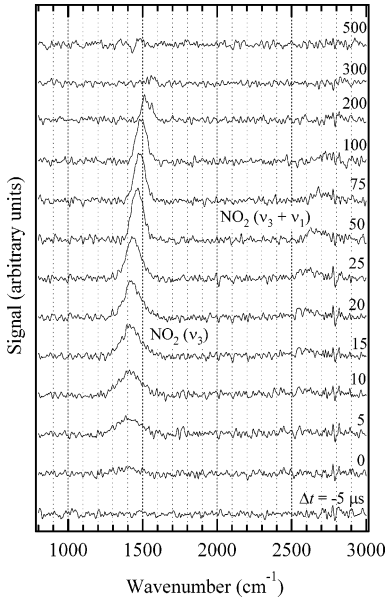

Figure 7. Infrared emission spectra at 8 cm^{-1} resolution following 248 nm photolysis of 7 mTorr chloropicrin in He at a total pressure of 391 mTorr, detected with a HgCdTe detector.

in previous spectra and is free of the beam splitter artifact at 8200 cm^{-1} seen in Figure 3. Similar to the photodissociation at 193 nm, the primary emission feature following chloropicrin and nitromethane photodissociation at 248 nm is the broad near-infrared feature assigned to the $NO_2[(\tilde{A}\ ^2B_2) \rightarrow (\tilde{X}\ ^2A_1)]$ transition. Spectra of nitromethane photodissociation at 248 nm (not shown) are qualitatively similar to those observed from chloropicrin photodissociation at 248 nm, although the total signal observed from nitromethane is significantly weaker.

The emission spectra following chloropicrin photodissociation at 248 nm with the HgCdTe detector, shown in Figure 7, are much simpler than the corresponding spectra at 193 nm (Figure 5). The only features are the two bands associated with $NO_2(\tilde{X}^2A_1)$, originating near 1400 and 2700 cm^{-1}, which rise slowly in intensity after photodissociation. We do not observe the NO band near 1820 cm^{-1}, which is of comparable intensity to the ν_3 band of NO_2 in Figure 4. Furthermore, the higher energy peak (near 1600 cm^{-1}) of the bimodal vibrational distribution in the ν_3 band of NO_2 is not present at 248 nm. The emission spectrum following chloropicrin photodissociation at 248 nm strongly resembles the emission spectrum of nitromethane following 193 nm photodissociation.

266 nm Photodissociation. When chloropicrin is photodissociated at 266 nm (Figure 8), we observe the same infrared emission bands as when chloropicrin is photodissociated at 248 nm. Because of the much lower signal levels at this wavelength, the emission is observed only with the more sensitive InSb detector, which cannot detect the strong ν_3 fundamental of NO_2. The broad near-infrared feature assigned to the $NO_2[(\tilde{A}\ ^2B_2) \rightarrow (\tilde{X}\ ^2A_1)]$ transition is again the primary feature, and the infrared emission observed at 2700 cm^{-1} is again assigned to the $\nu_3 + \nu_1$ combination band of $NO_2(\tilde{X}^2A_1)$. The 2700 cm^{-1} band also appears to be more intense relative to the $NO_2[(\tilde{A}\ ^2B_2) \rightarrow \tilde{X}\ ^2A_1]$ transition, as compared to the emission observed following photodissociation of chloropicrin at 248 nm, shown in Figure 6.

Infrared emission is also observed when nitromethane is excited at 266 nm, but the signal is too weak to acquire time-resolved spectra. The signal is 10 times lower for nitromethane as compared to chloropicrin under the same conditions. On the basis of the similarity of the chloropicrin and nitromethane fragment emission spectra at 248 nm and the thermodynamically available channels for nitromethane (see Figure 2), it is likely that nitromethane also photodissociates to produce $CH_3 + NO_2(\tilde{A}\ ^2B_2)$ at 266 nm.

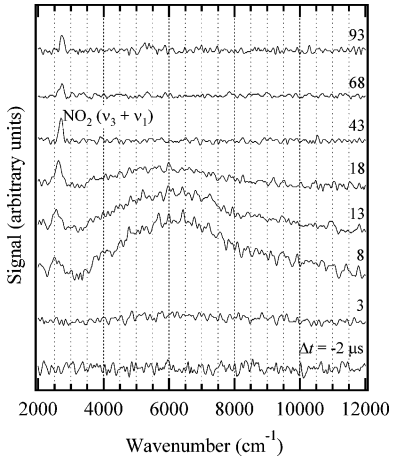

Figure 8. Infrared emission spectra at 64 cm^{-1} resolution following 266 nm photolysis of 8 mTorr chloropicrin in He at a total pressure of 600 mTorr, detected with an InSb photodiode.

Discussion

Nitromethane. For nitromethane photodissociated at 193 or 248 nm, the primary feature in the emission spectrum following photodissociation is the broad near-infrared band assigned to the $NO_2[(\tilde{A}\ ^2B_2) \rightarrow \tilde{X}\ ^2A_1]$ transition. This emission is consistent with cleavage of the C−N bond to produce electronically excited NO_2, which is the major channel observed by Blais[3] and Butler et al.[4] for nitromethane dissociation at 193 nm:

$$CH_3NO_2 \rightarrow CH_3 + NO_2(\tilde{A}\ ^2B_2)$$

Our time-dependent spectra show that electronically excited $NO_2(\tilde{A}\ ^2B_2)$ is quenched to highly vibrationally excited $NO_2(\tilde{X}\ ^2A_1)$, which we observe through emission from the ν_3 and $\nu_1 + \nu_3$ bands of NO_2. This coupling is consistent with the strong nonadiabatic interaction between the ground state and the first excited states, which interact via the asymmetric stretch (ν_3).[7] For nitromethane photodissociated at 193 and 248 nm, the only midinfrared emission observed from NO_2 arises from this pathway. There is no evidence in our spectra that $NO_2(\tilde{X}\ ^2A_1)$ is a nascent product of nitromethane dissociation at 193 nm. These results suggest that nitromethane dissociation does not occur on the ground electronic surface but rather on an excited electronic state that is either purely repulsive or predissociative. This hypothesis is consistent with the 2005 theoretical work of Arenas et al., which proposes a radiationless decay through a conical intersection, which deactivates the electronically excited nitromethane and causes it to dissociate and form $CH_3 + NO_2(\tilde{A}\ ^2B_2)$.[21]

We do not observe any emission from the methyl radical that is produced along with NO_2 in nitromethane photodissociation. The absence of CH_3 signal is due in part to the detection limits of the experiment and is likely also a result of the dissociation dynamics. As shown in Table 1, the three infrared active bands of the methyl radical have small Einstein *A* coefficients, making them difficult to observe experimentally as compared to the much stronger transitions in the ν_3 band of $NO_2(\tilde{X}\ ^2A_1)$. In addition, the carbon center in nitromethane is tetrahedral, whereas the equilibrium geometry of the methyl radical is planar.

TABLE 1: Fundamental Frequencies (cm^{-1}) and Einstein *A* Coefficients (s^{-1})

	NO_2		CH_3		CCl_3		CCl_2O		ClNO		CCl_2		NO	
label	ν_i [b]	A_i [b]	ν_i [b]	A_i [c]	ν_i	A_i [c]	ν_i [b]	A_i [c]	ν_i [d]	A_i [c]	ν_i [d]	A_i [c]	ν_i [b]	A_i [b]
ν_1	1320	0.08	3004	0.0[a]	269[c]	0.0	1827	149	1842[e]	307	710	2.0	1876	12.5
ν_2	750	0.23	607	3.5	330[c]	0.0	567	0.7	415	0.8	329	0.0		
ν_3	1618	113	3161	6.4	480[c]	0.0	285	0.0	250	0.2	720	24.1		
ν_4			1402	0.7	898[b]	19.7	580	0.3						
ν_5							849	40						
ν_6							440	0.1						

[a] Infrared inactive mode. [b] Experimental value. [c] Ab initio value (B3LYP/cc-pVTZ). [d] CCSD(T)/TZ2P Ref. T. J. Lee 1993, 1994. An absorption at ~1847 cm^{-1} in cryogenic matricies has been assigned to NOCl in ref 34.

When nitromethane dissociates on an excited state that is repulsive along the C−N bond, the methyl radical geometry must change from tetrahedral to planar, implying that the majority of the vibrational energy deposited in the CH_3 fragment will reside in the ν_2 umbrella mode. Unfortunately, we cannot observe the umbrella mode because its vibrational frequency lies below our 800 cm^{-1} detection threshold.

Our results offer support for the reinterpretation by Lao et al.[5] of the minor channel observed by Butler et al.[4] following dissociation of nitromethane at 193 nm. Butler et al. observed a minor channel associated with very little translational energy release, suggesting that the minor channel might be due to internal conversion of nitromethane to its ground electronic state yielding ground state products. Lao et al.[5] proposed that this minor channel is in fact due to near threshold dissociation to produce $NO_2(2\ ^2B_2)$. If $NO_2(\tilde{X}\ ^2A_1)$ were the product of the minor channel, the small translational energy associated with this channel would lead to prompt emission from highly vibrationally excited $NO_2(\tilde{X}\ ^2A_1)$, which we do not observe from nitromethane. Although we cannot confirm the reassignment of Lao et al.[5] that the minor channel produces $NO_2(2\ ^2B_2)$, such an assignment is more credible than direct production of $NO_2(\tilde{X}\ ^2A_1)$, which would clearly be observable in our experiment.

For nitromethane at longer photodissociation wavelengths, the previous literature contains a number of disagreements. Our results at 248 nm are consistent with Spears and Brugge[8] (who observed vibrationally excited NO_2) rather than with those of Kwok et al.[9] (who observed no photofragments). We do not observe any OH radical, in agreement with Greenblatt et al.[12] For 266 nm photodissociation of nitromethane, a very small emission signal is observed. Although we cannot absolutely identify the species responsible for this emission, given the similarity of the emission observed following chloropicrin and nitromethane photodissociation at 248 nm, the single product channel observed for chloropicrin photodissociation at 266 nm, and the energetics at this wavelength shown in Figure 2, the emission is likely due to $NO_2(\tilde{A}\ ^2B_2)$ through the same channel observed for 248 and 193 nm photodissociation of nitromethane.

$$CH_3NO_2 \rightarrow CH_3 + NO_2(\tilde{A}\ ^2B_2)$$

Chloropicrin. For chloropicrin photodissociated at 193, 248, and 266 nm, the emission spectra observed indicate a major photodissociation channel that is analogous to nitromethane:

$$CCl_3NO_2 \rightarrow CCl_3 + NO_2(\tilde{A}\ ^2B_2)$$

In determining the environmental fate of chloropicrin, the $\pi^* \leftarrow n$ transition centered at 270 nm and extending beyond 400 nm[23,26] is of primary importance, because sunlight in the troposphere does not extend to wavelengths shorter than 295 nm. This work suggests that the only significant environmental channel for direct photodissociation of chloropicrin is cleavage of the C−N bond to produce $NO_2(\tilde{A}\ ^2B_2)$, which for chloropicrin is energetically accessible for wavelengths as long as 400 nm.

When chloropicrin is photodissociated at 193 nm, the midinfrared emission is more complex than that observed for any other system in this work (see Figure 5), indicating that there are dissociation channels active for chloropicrin photodissociation at 193 nm that are not active at longer wavelengths or in nitromethane photodissociation. In particular, the bands peaking at early times near 900, 1600, and 1820 cm^{-1} are distinct from the features observed for nitromethane or for longer photodissociation wavelengths.

The band at 900 cm^{-1} is assigned to the CCl_3 stretching band ($\nu_4 = 898$ cm^{-1}, $A_{calc} = 19.7$ s^{-1}), the only mode of CCl_3 that is above the 800 cm^{-1} detector cutoff of the HgCdTe detector. Unlike the planar methyl radical, the trichloromethyl radical from chloropicrin dissociation is a pyramidal C_{3v} radical; therefore, less excitation might be expected in its umbrella bending mode. Furthermore, CCl_3 is easier to detect because the Einstein *A* coefficient for the ν_4 mode is significantly larger than for any mode in the methyl radical, as shown in Table 1. Our observation of the CCl_3 radical further supports our assignment of the major photodissociation channel to

$$CCl_3NO_2 \rightarrow CCl_3 + NO_2(\tilde{A}\ ^2B_2)$$

The 1600 cm^{-1} band, which has a detector-limited rise time and a monotonic decay thereafter, is assigned to nascent $NO_2(\tilde{X}^2A_1)$ with only modest vibrational excitation. For chloropicrin photodissociation at 193 nm, therefore, we observe NO_2 from two channels: The first produces electronically excited $NO_2(\tilde{A}\ ^2B_2)$ that is quenched to vibrationally excited $NO_2(\tilde{X}^2A_1)$, whereas the second channel produces $NO_2(\tilde{X}^2A_1)$ as a nascent photoproduct but with much less vibrational excitation. Differences in the observed distributions are highlighted in Figure 9, where the initial NO_2 ν_3 band 5 μs after photodissociation is shown for chloropicrin and nitromethane. The emission for chloropicrin photodissociated at 193 nm clearly shows a strong peak associated with low vibrational excitation ($v_{3,max} \sim 2$) and a second band with greater vibrational excitation ($v_{3,nax} \sim 9$). Therefore, we propose that during 193 nm photodissociation, chloropicrin has a product channel distinct from its nitromethane analogue.

One explanation for this second channel is dissociation of a C−Cl bond ($D_0 = 70$ kcal/mol) arising from excitation of a possible $\sigma^* \leftarrow 3p\pi$ transition in which a lone pair electron on a chlorine atom is excited to an antibonding C−Cl σ^* orbital. According to our calculations (Figure 2), the CCl_2NO_2 radical could contain 78 kcal/mol of internal energy but on average would likely have somewhat less internal energy due to the deposition of energy into relative translation along a repulsive C−Cl bond coordinate. Nevertheless, it is likely that a significant fraction of the CCl_2NO_2 so formed will have sufficient internal

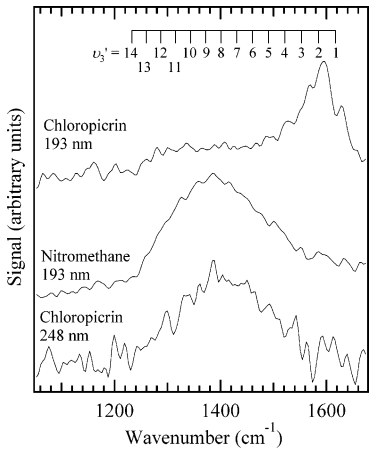

Figure 9. v_3 infrared band of NO_2 following 193 nm photolysis of chloropicrin and nitromethane and 248 nm photolysis of chloropicrin, taken at 8 cm^{-1} resolution, 5 ± 1 μs after the photolysis pulse. The vibrational origins of $\Delta v_1 = 0$, $\Delta v_2 = 0$, and $\Delta v_3 = -1$ vibrational transitions are shown, labeled by the initial vibrationally excited state.

energy to dissociate to $CCl_2 + NO_2(\tilde{X}\ ^2A_1)$.

$$CCl_3NO_2 \rightarrow CCl_2NO_2 + Cl$$

$$CCl_2NO_2 \rightarrow CCl_2 + NO_2(\tilde{X}\ ^2A_1)$$

This mechanism could quite plausibly produce $NO_2(\tilde{X}\ ^2A_1)$ promptly (on the time scale of our experiment) and with much less vibrational excitation than the $NO_2(\tilde{X}\ ^2A_1)$ produced by quenching of $NO_2(\tilde{A}\ ^2B_2)$ in the first channel, in agreement with our observations in Figure 5. Corroborating evidence for this mechanism could come from observation of the CCl_2 radical. Unfortunately, as shown in Table 1, all of the vibrational frequencies of the CCl_2 radical lie below our detection threshold of 800 cm^{-1}.

While the second step of this mechanism would support our spectra in Figure 5, we now consider signals that might arise from the initial C−Cl bond rupture. If a significant amount of CCl_2NO_2 radicals were stable with respect to dissociation, they would be detectable in our experiment. The CCl_2NO_2 radical has three vibrational modes calculated at the B3LYP/6-31G* level to lie in our spectral observation range with reasonably strong intensities: $\nu_{10} = 1061$ cm^{-1}, $A = 32$ s^{-1}; $\nu_{11} = 1305$ cm^{-1}, $A = 58$ s^{-1}; and $\nu_{12} = 1600$ cm^{-1}, $A = 45$ s^{-1}. There is no evidence of emission from any of these modes in Figure 5. Emission from spin−orbit excited Cl atoms at 882.3 cm^{-1} would not be detected in our apparatus due to the low strength of this transition ($A = 0.012$ s^{-1}). Therefore, if this mechanism is the origin of the prompt $NO_2(\tilde{X}\ ^2A_1)$ emission seen in Figure 5, it implies that most or all of the CCl_2NO_2 radicals have enough energy to dissociate. Detection of Cl atoms by other techniques would be useful in confirming the contribution of this mechanism.

At 248 nm, this two-step mechanism producing $NO_2(\tilde{X}\ ^2A_1)$ is energetically allowed but only by 6 kcal/mol. Therefore, even if this channel were active at 248 nm, it would be unlikely to produce any amount of vibrational excited NO_2 for detection with our apparatus. At 266 nm, this mechanism is not energetically feasible. Furthermore, while it is reasonable to assume that a $\sigma^* \leftarrow 3p\pi$ transition might contribute to one of the two UV absorption bands of chloropicrin shown in Figure 1, it is unlikely that this transition would contribute significant strength to both bands. Therefore, it seems reasonable to conclude that this dissociation mechanism does not contribute at 248 or 266 nm.

The band observed at 1820 cm^{-1} when chloropicrin is photodissociated at 193 nm is assigned to NO and arises from dissociation of NO_2 fragments that are born with internal energies above the ON−O dissociation limit. This assignment is confirmed with rotationally resolved measurements of NO taken at higher resolution. Although these spectra have poor signal-to-noise ratios, the rovibrational structure of NO could be clearly discerned, demonstrating the presence of NO. However, other possible products of chloropicrin photodissociation, listed in Table 1, could also contribute in this spectral region. To verify that this band is due primarily to NO, several time slices of the 1820 cm^{-1} band (at 8 cm^{-1} resolution) were fit to a simulated NO spectrum. The satisfactory fit indicates that no other contributions to the 1820 cm^{-1} band are required to reproduce the data. As shown in Table 1, the transitions in this region from phosgene and nitrosyl chloride have Einstein *A* coefficients more than an order of magnitude greater than NO. Therefore, if these other species were present, even as minor product channels, their emission would be significant as compared to the NO emission, and we would not be able to fit the observed emission using only NO basis functions. Therefore, we conclude that $CCl_2O + ClNO$ is not a primary product channel of chloropicrin photodissociation and that such products observed by Moilanen et al.[25] and Wade et al.[27] can be attributed to secondary reaction chemistry.

It is understandable that we observe NO following chloropicrin photodissociation and not following nitromethane photodissociation. First, for both chloropicrin and nitromethane photodissociated at 193 nm, it is possible to produce NO_2 above its dissociation threshold, as shown in Figure 2. However, because the C−N bond in chloropicrin ($D_0 = 41$ kcal/mol) is considerably weaker than the C−N bond in nitromethane ($D_0 = 62$ kcal/mol), more of the NO_2 produced will have sufficient internal energy to dissociate, and the resulting NO will have more internal energy (as much as 37 kcal/mol from chloropicrin vs 16 kcal/mol from nitromethane). This bond energy difference also makes the thermodynamics of nitromethane dissociation at 193 nm very similar to the thermodynamics of chloropicrin dissociation at 248 nm and may account for the strong resemblance of the emission spectra for those two photodissociation experiments. Butler et al.[4] found that >10% of the NO_2 produced from nitromethane photodissociation at 193 nm undergoes unimolecular dissociation. On the basis of the small amount of excess energy available for this channel, it seems likely that most of the resulting NO is produced in $v = 0$ and would therefore be unobserved in our emission spectra from nitromethane dissociation.

Conclusions

Step-scan FTIR emission spectroscopy was used to study the photodissociation of nitromethane and chloropicrin at 193, 248, and 266 nm. In all cases where spectra could be resolved, the major emission feature observed following both nitromethane and chloropicrin photodissociation can be explained by cleavage of the C−N bond to produce electronically excited NO_2:

$$CH_3NO_2 \rightarrow CH_3 + NO_2(\tilde{A}\ ^2B_2)$$

$$CCl_3NO_2 \rightarrow CCl_3 + NO_2(\tilde{A}\ ^2B_2)$$

Although infrared emission was observed when nitromethane was photodissociated at 266 nm, an infrared spectrum could not be collected. It is likely, however, that the infrared emission results from electronically excited NO_2, as in chloropicrin.

Two additional product channels are observed in our spectra of the photodissociation of chloropicrin at 193 nm. First, a significant fraction of the NO_2 produced from C−N bond cleavage has enough energy to dissociate, leading to the channel

$$CCl_3NO_2 \rightarrow CCl_3 + NO + O$$

Second, we observe some NO_2 in its ground electronic state with only modest vibrational excitation. One mechanism that is consistent with this observation is C−Cl bond cleavage, which could arise from a $\sigma^* \leftarrow 3p\pi$ transition in chloropicrin

$$CCl_3NO_2 \rightarrow CCl_2NO_2 + Cl$$

followed by unimolecular dissociation of the CCl_2NO_2 radical

$$CCl_2NO_2 \rightarrow CCl_2 + NO_2(\tilde{X}\ ^2A_1)$$

However, if this is the explanation for the $NO_2(\tilde{X}\ ^2A_1)$ with modest vibrational excitation that we observe following 193 nm dissociation, the $\sigma^* \leftarrow 3p\pi$ transition could not contribute at $\lambda > 295$ nm; therefore, this channel would not be environmentally significant.

At all wavelengths measured, the chloropicrin measurements strongly support an environmental photolysis mechanism in which the first step is cleavage of the C−N bond. The production of phosgene and nitrosyl chloride that is observed in environmental chambers[25] and cryogenic matrices[27] is therefore likely the result of secondary reactions between CCl_3 and NO_2.

Acknowledgment. We thank the referees for their helpful comments regarding dissociation mechanisms. This research is supported by the Division of Chemical Sciences, Geosciences, and Biosciences, the Office of Basic Energy Sciences of the U.S. Department of Energy. Sandia is a multiprogram laboratory operated by Sandia Corp., a Lockheed Martin Co., for the U.S. Department of Energy's National Nuclear Security Administration under contract DE-AC04-94AL85000. This work was also partially supported by the Petroleum Research Fund, Grant PRF#37424-GB4, administered by the American Chemical Society. We thank Gary Wilke and Howard Johnsen for technical assistance.

References and Notes

(1) Bayliss, N. S.; McRae, E. G. *J. Phys. Chem.* **1954**, *58*, 1006.
(2) Nagakura, S. *Mol. Phys.* **1960**, *3*, 152.
(3) Blais, N. C. *J. Chem. Phys.* **1983**, *79*, 1723.
(4) Butler, L. J.; Krajnovich, D.; Lee, Y. T.; Ondrey, G.; Bersohn, R. *J. Chem. Phys.* **1983**, *79*, 1708.
(5) Lao, K. Q.; Jensen, E.; Kash, P. W.; Butler, L. J. *J. Chem. Phys.* **1990**, *93*, 3958.
(6) Moss, D. B.; Trentelman, K. A.; Houston, P. L. *J. Chem. Phys.* **1992**, *96*, 237.
(7) Delon, A.; Jost, R. *J. Chem. Phys.* **1991**, *95*, 5686.
(8) Spears, K. J.; Brugge, S. P. *Chem. Phys. Lett.* **1978**, *54*, 373.
(9) Kwok, H. S.; He, G. Z.; Sparks, R. K.; Lee, Y. T. *Int. J. Chem. Kinet.* **1981**, *13*, 1125.
(10) Schoen, P. E.; Marrone, M. J.; Schnur, J. M.; Goldberg, L. S. *Chem. Phys. Lett.* **1981**, *90*, 272.
(11) Zabarnick, S.; Fleming, J. W.; Baronavski, A. P. *J. Chem. Phys.* **1986**, *85*, 3395.
(12) Greenblatt, G. D.; Zuckerman, H.; Haas, Y. *Chem. Phys. Lett.* **1986**, *134*, 593.
(13) Park, M. S.; Jung, K.-H.; Upadhyaya, H. P.; Volpp, H.-R. *Chem. Phys.* **2001**, *270*, 133.
(14) Dewar, M. J. S.; Ritchie, J. P.; Alster, J. *J. Org. Chem.* **1985**, *50*, 1031.
(15) McKee, M. L. *J. Phys. Chem.* **1989**, *93*, 7365.
(16) Nguyen, M. T.; Le, H. T.; Hajgato, B.; Veszpremi, T.; Lin, M. C. *J. Phys. Chem. A* **2003**, *107*, 4286.
(17) Hu, W.-F.; He, T-J.; Chen, D.-M.; Liu, F.-C. *J. Phys. Chem. A* **2002**, *106*, 7294.
(18) Mijoule, C.; Odiot, S.; Fliszar, S.; Schnur, J. M. *J. Mol. Struct.: THEOCHEM* **1987**, *149*, 311.
(19) Roszak, S.; Kaufman, J. J. *J. Chem. Phys.* **1991**, *94*, 6030.
(20) Arenas, J. F.; Otero, J. C.; Peláez, D.; Soto, J. *J. Chem. Phys.* **2003**, *119*, 7814.
(21) Arenas, J. F.; Otero, J. C.; Peláez, D.; Soto, J. *J. Chem. Phys.* **2005**, *122*, 084324.
(22) Leistra, M.; Crum, S. J. H. *Water, Air, Soil Pollut.* **1990**, *50*, 109.
(23) Atkinson, R. *Atmos. Environ.* **1990**, *24A*, 1.
(24) Allston, T. D.; Fedyk, M. L.; Takacs, G. A. *Chem. Phys. Lett.* **1978**, *60*, 97.
(25) Moilanen, K. W.; Crosby, D. G.; Humphrey, J. R.; Giles, J. W. *Tetrahedron* **1978**, *34*, 3345.
(26) Carter, W. P. L.; Luo, D.; Malkina, I. L. *Atmos. Environ.* **1997**, *31*, 1425.
(27) Wade, E. A.; Reak, K. E.; Parsons, B. F.; Clemes, T. P.; Singmaster, K. A. *Chem. Phys. Lett.* **2002**, *365*, 473.
(28) Clegg, S. M.; Parsons, B. F.; Klippenstein, S. J.; Osborn, D. L. *J. Chem. Phys.* **2003**, *119*, 7222.
(29) Orphal, J.; Dreher, S.; Voigt, S.; Burrows, J. P.; Jost, R.; Delon, A. *J. Chem. Phys.* **1998**, *109*, 10217.
(30) Donnelly, V. M.; Kaufman, F. *J. Chem. Phys.* **1977**, *66*, 4100.
(31) Frisch, M. J.; Trucks, G. W.; Schlegel, H. B.; Scuseria, G. E.; Robb, M. A.; Cheeseman, J. R.; Zakrzewski, V. G.; Montgomery, J. A.; Stratmann, R. E.; Burant, J. C.; Dapprich, S.; Millam, J. M.; Danniels, A. D.; Kudin, K. N.; Strain, M. C.; Farkas, O.; Tomasi, J.; Barone, V.; Cossi, M.; Cammi, R.; Mennucci, B.; Pomelli, C.; Adamo, C.; Clifford, S.; Ochterski, J.; Petersson, G. A.; Ayala, P. Y.; Cui, Q.; Morokuma, K.; Malick, D. K.; Rabuck, A. D.; Raghavarchari, K.; Foresman, J. B.; Cioslowski, J.; Ortiz, J. V.; Stefanov, B. B.; Liu, G.; Liashenko, A.; Piskorz, P.; Komaromi, I.; Gomperts, R.; Martin, R. L.; Fox, D. J.; Keith, T.; Al-Laham, M. A.; Peng, C. Y.; Nanayakkara, A.; Gonzalez, C.; Challacombe, M.; Gill, P. M. W.; Johnson, B.; Chen, W.; Wong, M. W.; Andres, J. L.; Gonzalez, C.; Head-Gordon, M.; Replogle, E. S.; Pople, J. A. *Gaussian 98*, Revision A.6; Gaussian: Pittsburgh, PA, 1998.
(32) Rogers, E. E.; Abramowitz, S.; Jacox, M. E.; Milligan, D. E. *J. Chem. Phys.* **1970**, *52*, 2198.
(33) Huber, K. P.; Herzberg, G. Constants of diatomic molecules; data prepared by Gallagher, J. W., Johnson, R. D. In *NIST Chemistry WebBook, NIST Standard Reference Database 69*; Linstrom, P. J., Mallard, W. G., Eds.; National Institute of Standards and Technology: Gaithersburg, MD, 2003; http://webbook.nist.gov.
(34) Jacox, M. E. Vibrational and electronic energy levels of polyatomic transient molecules. In *NIST Chemistry WebBook, NIST Standard Reference Database 69*; Linstrom, P. J., Mallard, W. G., Ed.; National Institute of Standards and Technology: Gaithersburg, MD, 2003; http://webbook.nist.gov.
(35) Afeefy, H. Y.; Liebman, J. F.; Stein, S. E. Neutral thermochemical data. In *NIST Chemistry WebBook, NIST Standard Reference Database 69*; Linstrom, P. J., Mallard, W. G., Eds.; National Institute of Standards and Technology: Gaithersburg, MD, 2003; http://webbook.nist.gov.
(36) Ochterski, J. W.; Petersson, G. A.; Montgomery, J. A. *J. Chem. Phys.* **1996**, *104*, 2598.